

Fibrosis of the Choroid Plexus Filtration Membrane

John W. Prineas, MD, John D. E. Parratt, MD, PhD, and Paul D. Kirwan, PhD

Abstract

We report a previously undescribed inflammatory lesion consisting of deposition of activated complement (C3d and C9neo) in association with major histocompatibility complex type II (MHC2)-positive activated microglia in choroid plexus villi exhibiting classical fibrous thickening of the pericapillary filtration membrane. The proportion of villi affected ranged from 5% to 90% in 56 adult subjects with diseases of the CNS and 11 subjects with no preexisting disease of the CNS. In 3 of the 4 children studied, 2% or less of examined villi showed stromal thickening, complement deposition, and the presence of MHC2-positive microglia; in adults, the proportion of villi affected increased with age. Other features of the lesion included loss of capillaries and failure by macrophages to clear extracellular particulate electron-dense material by clathrin-mediated phagocytosis. This choroid plexus lesion may relate pathogenetically to age-related macular degeneration and to Alzheimer disease, 2 other conditions with no known risk factors other than increasing age. All 3 conditions are characterized by the presence of damaged capillaries, inflammatory extracellular aggregates of mixed molecular composition and defective clearance of the deposits by macrophages.

Key Words: Alzheimer disease, Choroid plexus, Complement, Macular degeneration, Multiple sclerosis.

INTRODUCTION

In a previous immunohistochemical study, we reported the chance observation that choroid plexuses in the lateral, third and fourth ventricles in 6 patients with neuromyelitis optica (NMO) showed a striking accumulation of activated complement (C3d, C9neo) within the normally empty perica-

pillary space of the choroid plexus filtration membrane in all 18 specimens examined (1) (Figs. 1, 2). In clinically active cases of NMO examined at autopsy, activated complement is deposited along the glial limiting membrane at the surface of the brain and spinal cord and around blood vessels but there is nothing known about NMO that explains the presence of activated complement in choroid plexus villi (1–3).

The complement system comprises a group of pro-inflammatory proteins that are activated and deposited at sites of inflammation associated with antibody-mediated and innate immune reactions. C3d and C9neo are forms of activated complement that can be identified immunohistochemically using specific antibodies. Their presence in NMO choroid plexus villi indicates the possibility of an inflammatory lesion in the choroid plexus in this disease.

In this study, in addition to investigating the immunopathology and electron microscopic features of the choroid plexus lesion in NMO, choroid plexuses in patients with multiple sclerosis (MS) and other inflammatory and non-inflammatory conditions affecting the CNS were examined for evidence of complement deposition.

Because the unusual location of the NMO lesion, i.e. within the pericapillary space of a filtration membrane, might be a factor related to the cause of the lesion, we examined, by electron microscopy (EM), the retinal filtration membrane in a patient with pathologically defined age-related macular degeneration (AMD) and the glomerular filtration membrane in 11 patients with immune complex and other diseases of the kidney.

MATERIALS AND METHODS

Patients

The study was approved by the University of Sydney committee on human experimentation. Choroid plexus tissue from 71 subjects was studied immunohistochemically for inflammatory cells and IgG, C3d and C9neo immunoreactivity, 60 with diseases of the CNS (29 females and 31 males, median age 45 years, range 6–73 years) (Tables 1, 2) and 11 adults with no preexisting CNS disease.

Histopathology

Archival paraffin-embedded blocks obtained at routine autopsy containing choroid plexus tissue were selected for study. Whole brains had been fixed in buffered formalin on average for 2 weeks. Some were sliced and fixed for 2 days at

From the The Institute of Clinical Neurosciences and the Nerve Research Foundation, Department of Medicine, University of Sydney, NSW, Australia (JWP, JDEP), Department of Neurology, Royal North Shore Hospital, St. Leonards, Sydney, NSW, Australia (JDEP) and Electron Microscope Unit, Department of Anatomical Pathology, Concord Repatriation Hospital, Concord, Sydney, NSW, Australia (PDK)

Send correspondence to: Dr. J.W. Prineas, Room 711-MO2F, Brain and Mind Research Institute, University of Sydney, 94 Mallet Street, Camperdown, NSW 2050, Australia; E-mail: john.prineas@sydney.edu.au

Funding: Grants were received from Multiple Sclerosis Research Australia (J.W.P. and J.D.E.P.) the National Multiple Sclerosis Society (J.W.P.), the Nerve Research Foundation, University of Sydney (J.W.P. and J.D.E.P.), the NSW Ministry for Science and Medical Research (J.W.P.), and the National Multiple Sclerosis Society (United States RG2731-A-8).

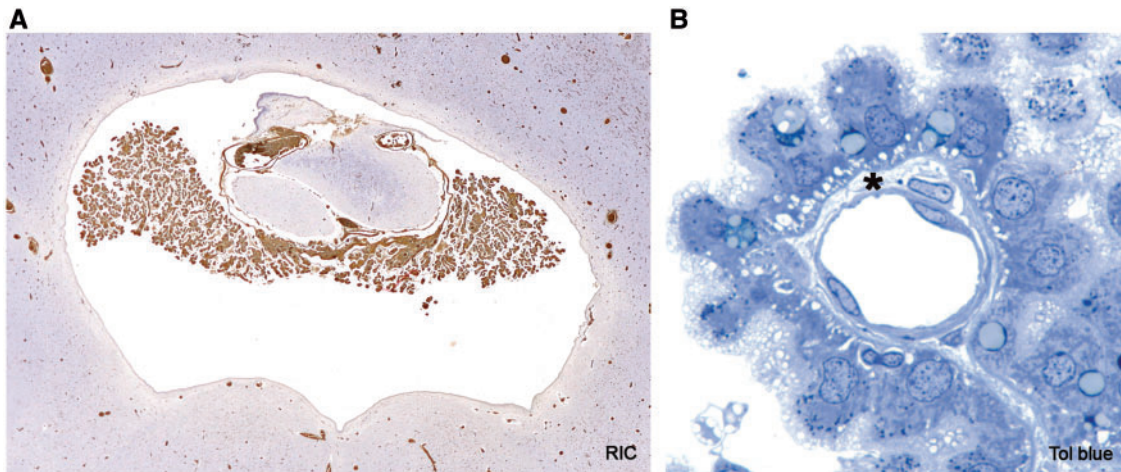


FIGURE 1. Choroid plexus **(A)** A choroid plexus in the roof of the fourth ventricle immunostained using a labeled lectin that stains vascular endothelium a brownish color. The staining pattern reflects the fact that choroid plexuses are composed largely of massed capillaries. **(B)** A choroid plexus capillary located within a normal-appearing choroid plexus villus. The asterisk is located within the pericapillary space of the filtration membrane. Vacuoles at the base of each epithelial cell represent extracellular fluid-filled cisterns located amongst epithelial cell foot processes as shown in Figure 2. Human tissue: **A**, RCA-1, $\times 5$; **B**, Semi-thin section, toluidine blue, $\times 900$.

4°C in buffered 4% paraformaldehyde. Autopsy intervals ranged from 2 h to in most cases 1–3 days. Paraffin sections, 4- to 10- μ m thick, were mounted on Ultrafrost slides (Thermo Scientific) and stained using Luxol fast blue–periodic acid Schiff (LFB-PAS), Bodian’s silver stain for axons, and hematoxylin and eosin (H&E). Other stains used in selected cases included *Ricinus communis* agglutinin-1 (RCA-1) for microglia, macrophages and vascular endothelial cells, and Congo red birefringence for amyloid.

Immunohistochemistry

Following microwave antigen retrieval (citrate buffer pH 6), and treatment to block non-specific staining, deparaffinized 4- to 10- μ m-thick sections were incubated with optimally diluted primary antibody for 30 min at room temperature or for 3 days at 4°C, as previously described in (1). Primary antibodies selected for use included not only those directed at inflammatory mediators but also antibodies that recognized putative myelin and other autoantigenic determinants that might be detectable in antigen-antibody complex deposits. The primary antibodies used recognized: IgG (polyclonal, Organon Teknika, Westchester, PA); IgM (polyclonal, Dako, Carpinteria, CA); C3d (polyclonal, Dako) and C9neo (C5b9, B7 [B.P Morgan, Cardiff, UK]); and glial fibrillary acidic protein (GFAP) (GF12-24, Millipore Corporation, Billerica, MA). Primary antibodies were detected using polymer-coated, horseradish peroxidase-conjugated secondary antibodies (EnVision and Advance™, DakoCytomation Inc., Carpinteria, CA) with 3, 3'-diaminobenzidine as the chromogen. Selected sections were stained for aquaporin-4 (AQP4), myelin oligodendrocyte glycoprotein (MOG), CNPase, CD45, CD68, major histocompatibility complex type II (MHC2) and for lymphocytes (CD4, CD8 and UCHL-1).

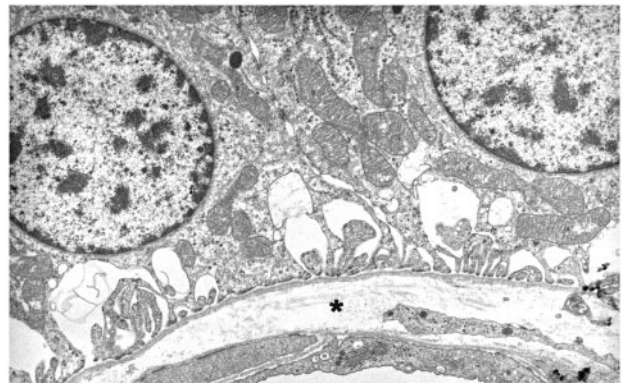


FIGURE 2. The filtration membrane. The asterisk is located in the pericapillary space of the filtration membrane. Other components of this complex structure are seen below and above the asterisk. Below is the fenestrated endothelium of the capillary and its very thin basal lamina. Above is the basal lamina of the epithelium together with the tips of epithelial cell foot processes and large extracellular fluid-filled cisterns that bulge into the base of each of the 2 epithelial cells. Human tissue: electron micrograph, $\times 7000$.

Renal biopsies from patients with known immune complex diseases served as positive controls for C3d and C9neo. Negative controls included omission of the primary antibody and use of non-reactive immunoglobulin.

To quantify damage to the choroid plexus filtration membranes (interstitial fibrosis), 100 villi in each case were examined for pericapillary space fibrosis and nodule formation using routinely stained sections (H&E, LFB-PAS). To determine the proportion of villi immunoreactive for complement in each patient, a semiquantitative assessment of pericapillary space C3d immunoreactivity was assessed using the

TABLE 1. Clinical Data on Patients 1–30

| Case | Sex/age (years) | Diagnosis | Duration (MS) | C3d | Diseased villi/100 |
|------|-----------------|-------------|---------------|-------|--------------------|
| 1 | M 30 | syphilis | | 1 + | 53 |
| 2 | M 59 | MS | “chronic” | | 22 |
| 3 | M 11 | ALD | | 0 | 2 |
| 4 | F 14 | MS | 9 months | 1 + | 18 |
| 5 | F 53 | MS | 24 months | 2 ++ | |
| 6 | F 55 | subdural | | | 22 |
| 7 | F 6 | astrocytoma | | | 0 |
| 8 | F 39 | MS | 5 years | 1 + | 17 |
| 9 | M 52 | infarct | | 1 + | 19 |
| 10 | F 51 | MS | 15 years | | 5 |
| 11 | F 65 | ADEM | | 2 ++ | 45 |
| 12 | M 18 | MS | 10 years | | 37 |
| 13 | F 42 | metastases | | | 6 |
| 14 | M 55 | MS | “chronic” | 3 +++ | 33 |
| 15 | M 21 | SSPE | | 2 ++ | 67 |
| 16 | M 55 | metastases | | | 22 |
| 17 | M 68 | syphilis | | | 90 |
| 18 | M 21 | MS | 49 months | | 11 |
| 19 | F 40 | MS | 10 weeks | 1 + | 27 |
| 20 | M 45 | MS | 10 years | 2 ++ | 37 |
| 21 | M 27 | MS | 14 months | | 53 |
| 22 | F 50 | MS | 22 years | | 27 |
| 23 | F 39 | MS | 14 years | | 33 |
| 24 | F 49 | NMO | | 1 + | |
| 25 | M 32 | MS | 9 months | 1 + | 20 |
| 26 | M 46 | ADEM | | 1 + | 23 |
| 27 | F 38 | MS | “chronic” | | 12 |
| 28 | M 14 | MS | 18 days | 1 + | 6 |
| 29 | M 49 | MS | 3 months | 2 ++ | 49 |
| 30 | F 28 | MS | 33 months | 1 + | 18 |

Disease duration refers to duration of symptoms prior to death in patients with MS. C3d: semi-quantitative assessment of extent of stromal C3d immunoreactivity: 0, absent; +, sparse; ++, moderate; +++, extensive. Diseased villi: 100 villi in each case examined for stromal thickening including nodule formation. Each number represents the number per 100 counted showing widening of the filtration membrane due to stromal fibrosis or the presence of a nodule. ADEM, acute disseminated encephalomyelitis; F, female; M, male; NMO, neuromyelitis optica.

following scale: 0 = absent; + = sparse; ++ = moderate; +++ = extensive. MHC2-positive microglia/macrophages were recorded as present or absent in affected villi (+ to +++ C3d immunoreactivity). All assays were conducted by blinded observers. The results are shown in Tables 1 and 2.

Electron Microscopy

Six blocks of choroid plexus tissue adequately fixed for EM from the lateral and fourth ventricles were available from a typical case of MS, a woman aged 39 years with a 14-year history and no known disease other than MS (4). Retinal tissue from the same case revealed changes typical of pathologically defined AMD. It was used to examine and illustrate points of resemblance between retinal and choroid plexus filtration membranes.

TABLE 2. Clinical Data on Patients 31–60

| Case | Sex/age | Diagnosis | Duration (MS) | C3d | Diseased villi/100 |
|------|---------|--------------|---------------|-------|--------------------|
| 31 | M 66 | NMO | | 3 +++ | 39 |
| 32 | F 70 | MS | 21 days | 3 +++ | 41 |
| 33 | F 48 | NMO | | 3 +++ | 32 |
| 34 | M 8 | SSPE | | | 2 |
| 35 | M 34 | MS | 45 months | 2 ++ | 50 |
| 36 | F 49 | NMO | | 1 + | 9 |
| 37 | M 59 | NMO | | 2 ++ | 31 |
| 38 | M 40 | MS | 8 years | | 10 |
| 39 | F 52 | MS | 12 years | 3 +++ | 33 |
| 40 | F 21 | MS | 3 years | | 15 |
| 41 | M 34 | MS | 34 years | 2 ++ | 37 |
| 42 | M 62 | hemorrhage | | | 11 |
| 43 | M 54 | MS | | 2 ++ | 28 |
| 44 | M 25 | MS | 29 days | 1 + | 8 |
| 45 | M 11 | PML | | | 10 |
| 46 | F 62 | MS | 16 years | | 19 |
| 47 | F 45 | MS | 4 weeks | 2 ++ | 12 |
| 48 | M 71 | MS | 26 years | 3 +++ | 71 |
| 49 | F 55 | MS | 16 years | | 11 |
| 50 | M 30 | angioma | | | 10 |
| 51 | F 27 | MS | 49 months | 2 ++ | 15 |
| 52 | M 43 | MS | 14 years | | 25 |
| 53 | M45 | MS | 2 weeks | 2 ++ | 39 |
| 54 | F 19 | MS | 1 week | 1 + | 44 |
| 55 | F 55 | syphilis | | | 17 |
| 56 | M 36 | MS | 3 years | 1 + | 18 |
| 57 | F 36 | subdural | | | 28 |
| 58 | F 53 | subdural | | | 14 |
| 59 | F 73 | encephalitis | | | 23 |
| 60 | F 53 | MS | 10 years | | 44 |

Disease duration refers to duration of symptoms prior to death in patients with MS. C3d: semi-quantitative assessment of extent of stromal C3d immunoreactivity: 0, absent; +, sparse; ++, moderate; +++, extensive. Diseased villi, 100 villi in each case examined for stromal thickening including nodule formation. Each number represents the number per 100 counted showing widening of the filtration membrane due to stromal fibrosis or the presence of a nodule. F, female; M, male; NMO, neuromyelitis optica; PML, progressive multifocal leukoencephalopathy.

To compare changes in choroid plexus villi with fine structural changes in renal filtration membranes in patients with an age-related renal disease (fibrillary glomerulonephritis [FG]), diagnostic renal biopsies from patients with immune complex disease of the kidney and with other renal diseases (in which the diagnosis was established by routine immunohistochemical procedures and EM) were reviewed. These renal conditions included lupus nephritis, membranous glomerulonephritis, post-infectious glomerulonephritis associated with chronic bacterial infections, IgA disease, age-related FG, Alport syndrome, age-related focal segmental glomerulosclerosis (a disease of the elderly thought to be ischemic in origin), diabetic glomerulosclerosis, dense deposit disease and minimal lesion glomerulonephropathy.

Choroid plexus tissue for EM was fixed in 3% glutaraldehyde and 2% osmium tetroxide. Sections were stained with uranyl acetate and lead citrate.

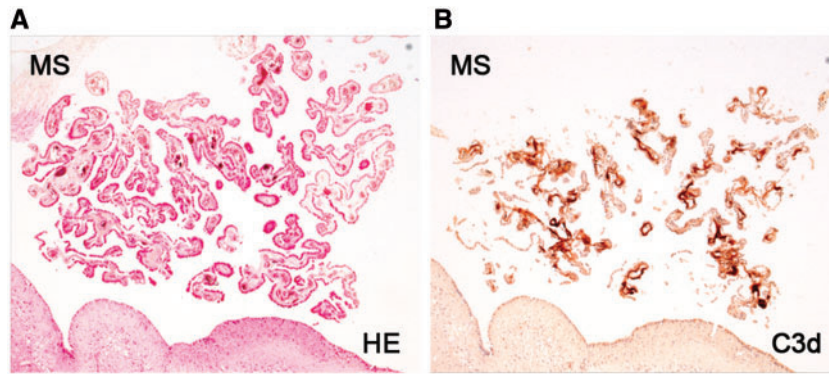


FIGURE 3. Complement deposition in the choroid plexus of a 45-year-old male patient with MS. **(A, B)** A lateral ventricle choroid plexus stains positively for activated complement. **A**, H&E; **B**, C3d. Magnifications: **A, B**, $\times 25$.

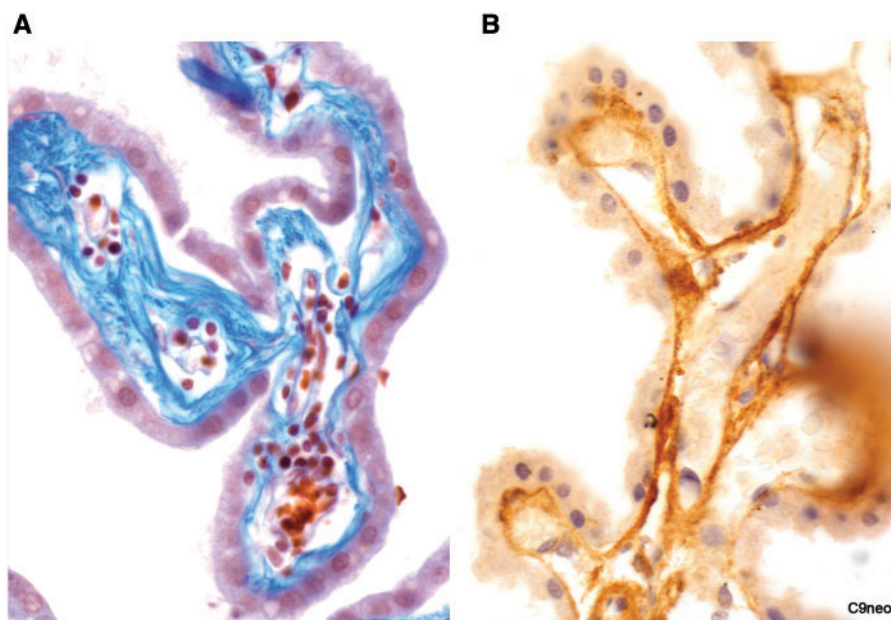


FIGURE 4. Interstitial fibrosis. **(A)** The pericapillary space in each of the 3 villi is occupied by a thick layer of connective tissue. The capillaries have reduced diameters. **(B)** The relatively narrow perivascular space of 3 villi and the connecting portion of the frond is occupied by a thin layer of connective tissue that is immunostained positively for C9neo. **A**, Mallory trichrome, $\times 460$; **B**, C9neo, $\times 520$.

Statistical Analysis

Statistical analyses of villous fibrosis versus age, villous fibrosis versus disease duration, and villous fibrosis versus complement deposition were performed using SPSS version 22.0.

RESULTS

Complement and Immunoglobulins

Choroid plexuses examined immunohistochemically (i.e. both those with [$n = 33$, Tables 1, 2] and those without [$n = 11$] CNS disease), stained positively for activated complement (C3d and C9neo) (Fig. 3). The single case with no evidence of complement deposition in the choroid plexus was

the only child in the immunohistochemistry series, an 11-year-old boy with adrenoleukodystrophy (Case 3, Table 1).

Serial sections showed that both C9neo and C3d immunoreactivity localized to filamentous and amorphous, pale or faintly eosinophilic material that was present, often as a nodule, within the normally empty pericapillary space of the villous filtration membrane; the proportion of affected villi staining positively for C9neo was approximately the same as the proportion that stained positively for C3d (Figs. 4–7). The same material stained positively with silver stains (Fig. 8B) but was negative for amyloid.

Nodules were capped by thickened PAS-positive subepithelial basal laminae that intruded into the overlying epithelium. Expansion of the nodule occurred at the expense of the capillary, which was reduced in diameter or absent.

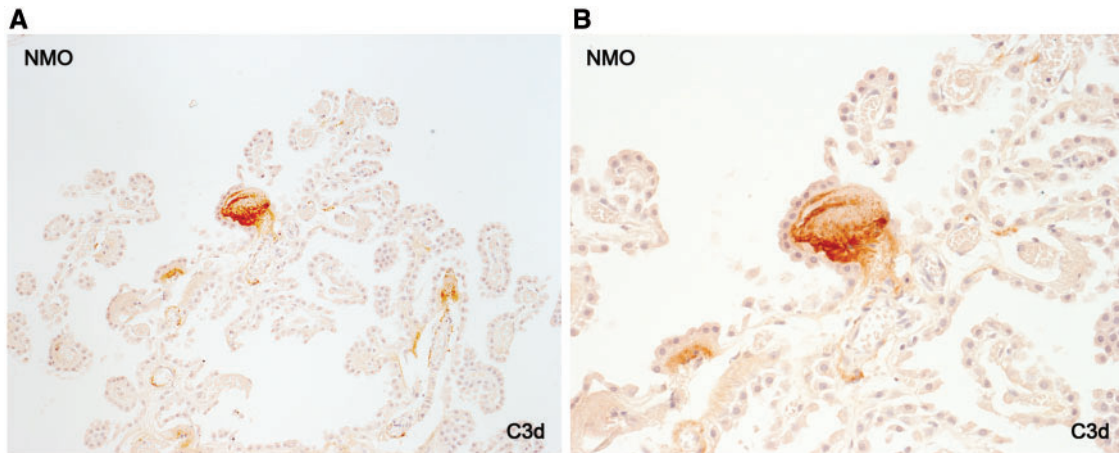


FIGURE 5. Early deposition of complement in the choroid plexus of a patient with NMO. **(A, B)** Complement immunoreactivity (C3d) is restricted to a single large villous nodule. **A**, $\times 90$; **B**, $\times 180$.

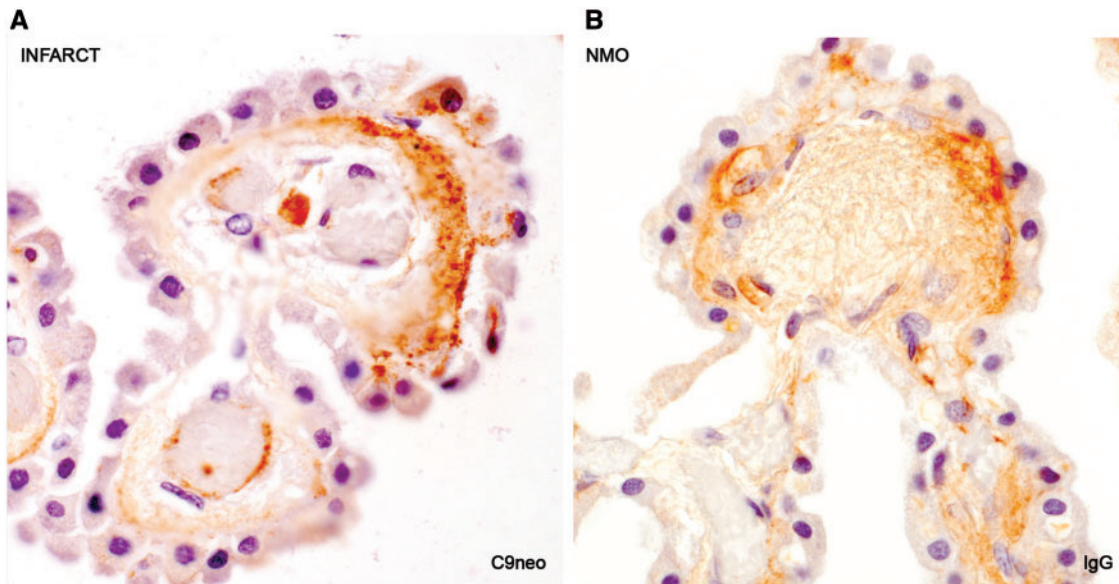


FIGURE 6. Complement and IgG deposits. Choroid plexus perivascular nodules (stromal fibrosis) in patients with cerebral infarction **(A)** and NMO **(B)**. Immunoreactivity is restricted to material located within the fibrosed pericapillary space. **A**, C9neo, $\times 560$; **B**, IgG, $\times 570$.

IgG immunoreactivity, which was present in 50% of the cases, appeared as a diffuse or granular band towards the apex of a nodule (Figs. 6B, 8C). Importantly, the pattern was the same in patients with MS, in those with other inflammatory neurological diseases including NMO, and in patients with non-inflammatory diseases. EM of choroid plexus tissue in a patient with longstanding MS and extensive interstitial fibrosis of the choroid plexus (IFCP) showed no EM evidence of immune complex deposition.

Diffusely thickened as well as nodular areas of fibrous thickening of the pericapillary space were unstained with other primary antisera including antibodies directed against IgM, β -lipoprotein, GFAP, MOG and AQP4. They stained positively for λ and κ light chains and occasionally also for fibrinogen.

Epithelial cell cytoplasm was positive with variable intensity for IgG and κ and λ light chains, AQP 4 and transferrin. Ring-like bodies sometimes present in the choroid plexus epithelium (“silver rings of Biondi”) stained positively for MOG.

Inflammatory Cells

MHC2-positive microglia/macrophages were present in pericapillary spaces of all villi examined where there was deposition of complement and stromal fibrosis, including the occasional villous seen containing a mineral inclusion (Fig. 9). Lymphocytes were rarely seen. An exception was a patient with MS who had some months prior to death had received injections of an extract of pig brain. In this patient, UCHL-1-

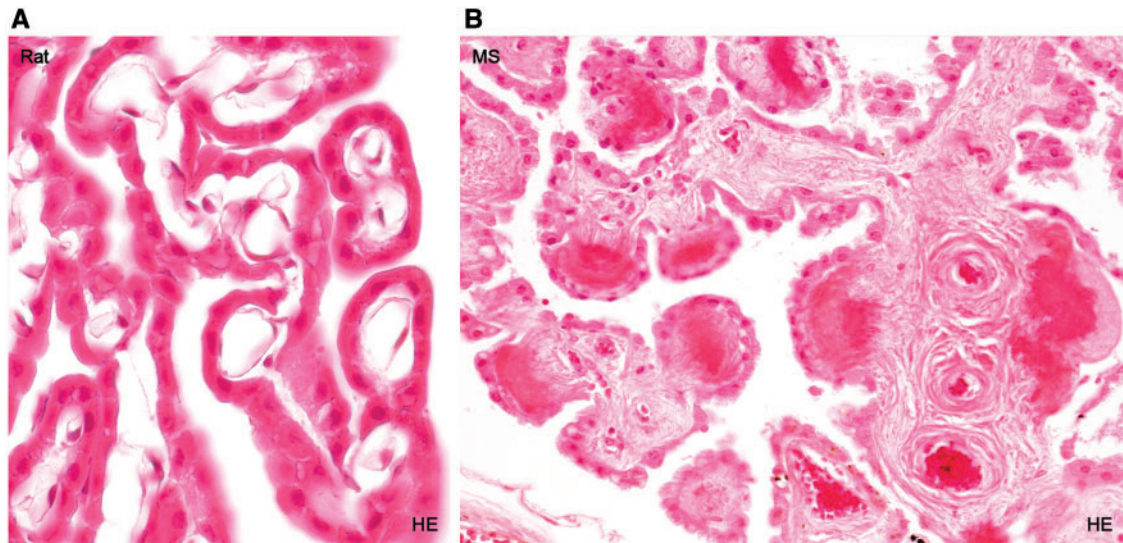


FIGURE 7. Rat and human choroid plexus villi. **(A)** The choroid plexus of a young rat showing each villous entirely occupied by a large capillary. The pericapillary space is narrow and without discernible contents. **(B)** A choroid plexus in a 71-year-old male patient with MS in which more than half the number of villi present exhibit narrowing or loss of capillaries together with marked stromal fibrosis. **A**, Frozen section, H&E, $\times 430$; **B**, paraffin section, H&E, $\times 200$.

positive lymphocytes were numerous throughout the choroid plexus as well as in typical MS plaques and experimental autoimmune encephalomyelitis-like lesions present throughout the brain (Fig. 9D). UCHL-1 lymphocytes (CD45RO-positive T cells) are a particular class of activated memory T cells capable of responding to antigens.

Where CD68-positive cells were seen close to complement-positive deposits, there was no evidence of uptake of the material by putative phagocytes. In contrast, where fresh MS lesions or recent ischemic infarcts containing numerous macrophages were present in cerebral tissue remote from the ventricles, CD68-positive phagocytes were distended with endocytosed complement-positive cell debris. We interpret this as an indication that in affected choroid plexus villi there may be some local impediment to phagocytosis of extracellular complement-positive material.

Interstitial Fibrosis

Widening of the pericapillary space of individual villi by filamentous and amorphous material was assessed using a semiquantitative scale as follows: + = no, equivocal or slight widening; ++ = moderate widening; +++ = nodular widening. Villi rated ++ or +++ were counted as fibrosed whereas villi rated + were rated as not fibrosed. Assessment was by a blinded observer (J.W.P.) using coded slides. Fibrosis was detected in all but one of 58 choroid plexuses examined using routine neuropathological stains from patients with CNS disease (mean number of villi affected per hundred examined: 26.206 ± 18.244 (SD) (Tables 1, 2). The exception was a 6-year-old girl with an astrocytoma in whom all villi examined showed no fibrosis (Case 7, Table 1). The findings were similar in all 11 adult subjects (not age-matched) without CNS disease (mean number of villi affected per 100 examined 36.45 ± 19.66 [SD]).

The relationship of age to number of villi with ++ or +++ fibrosis was examined in a cohort of 113 subjects: 53 MS patients, 43 patients with other neurological diseases, and 17 without pre-existing CNS disease. The difference in mean number of villi fibrosed per 100 examined in each case did not differ significantly among MS patients (mean 29.6 [95% CI 23.2–34.9]), other neurological disease patients (mean 33.7 [95% CI 25.1–41.2]), and the non-neurological disease group (mean 35.7 [95% CI 22.2–49.2]). Simple linear regression showed that age was associated with the number of villi affected, i.e. that age was a significant covariate with Beta = 0.327 and $p = 0.005$, which means that for every increase in age of 0.33 years there is a 1% increase in villi affected. EM of affected villi in 6 blocks of tissue from the single case examined showed the nodules to be composed of collagen together with occasional deposits of unusual, irregularly shaped, electron-dense particles identical to those described in previously reported EM studies of age-related choroid plexus stromal fibrosis and psammoma body formation (5). The particles lay in close contact with process-bearing cells located within the widened pericapillary space (Fig. 10A, B, F), and appeared to form in association with collagen fibers (Fig. 10E). Importantly, there was no evidence of phagocytosis although the material was enveloped by cytoplasmic processes with what appeared to be clathrin-coated pits at points of contact (Fig. 10C, D).

Complement Immunoreactivity and Stromal Fibrosis

To determine the relationship between stromal fibrosis and inflammation, we analyzed findings in 21 patients with MS, the largest group in the study with the same pre-existing CNS disease and in whom both C3d stained sections as well as sections assessed for stromal fibrosis were available (Tables 1

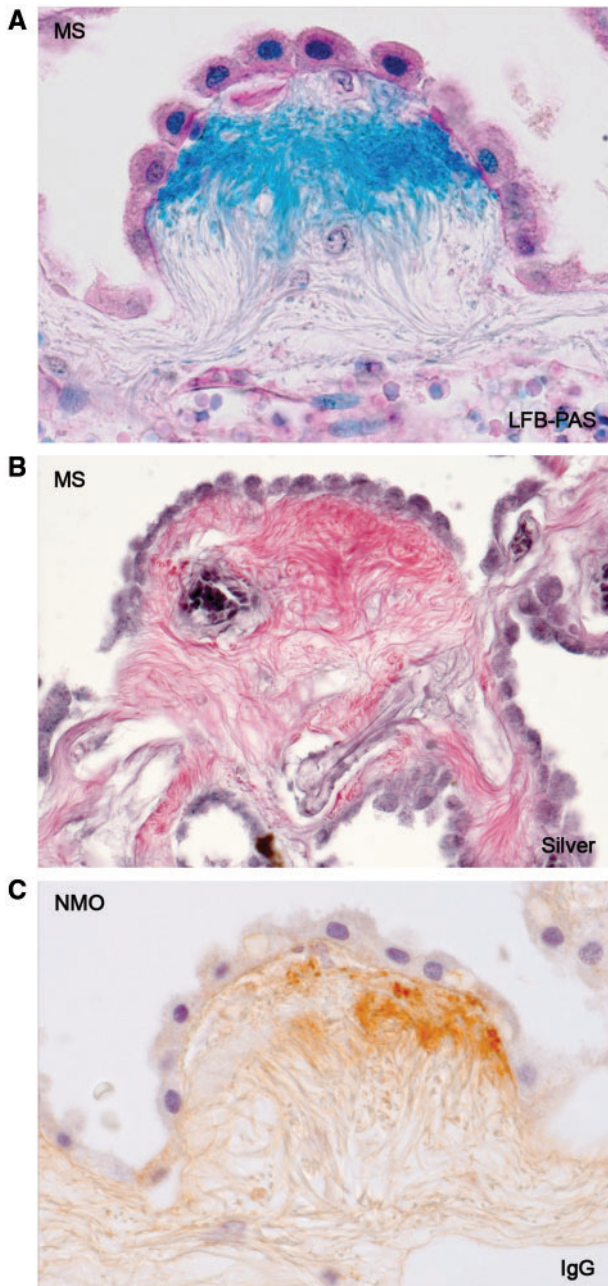


FIGURE 8. Stromal fibrosis nodules in choroid plexus of MS and NMO patients. Nodules occupy most of the space normally occupied by a capillary. **A**, MS, Luxol fast blue-PAS, $\times 460$; **B**, MS, Bodian's silver stain, $\times 210$; **C**, NMO, IgG immunohistochemistry, $\times 450$.

and 2). Simple linear regression analysis showed a significant correlation between the number of villi with stromal fibrosis and C3d staining ($r=0.6$, $p=0.004$ univariate). Also, a significant correlation was found between the number of diseased villi and age of the patient ($r=0.6$, $p=0.004$ univariate). Despite univariate significant associations between age, disease duration and number of affected villi (when age and disease duration were entered into an analysis of variance

model), age remained a significant predictor of the number of diseased villi ($p=0.05$) and disease duration (measured in months) did not ($p=0.178$).

Choroid Plexus Epithelium

By light microscopy, the epithelium appeared normal except where the villous was occupied by a large nodule. In the latter case, the small cavities normally visible at the base of each epithelial cell were reduced in size or absent (Fig. 11). As previously reported (6), EM showed that the basal cavities in unaffected villi are formed by elaborately folded plasma membranes producing regions in each epithelial cell of increased surface area.

The loss of cavities was associated with an increase in thickness of the subepithelial basal lamina and the formation of ridge-like intrusions that extended into the zone of attenuated epithelial folds and foot processes, as described by others in (6, 7) (Fig. 12).

Perivascular Spaces in the Cerebrum

Complement (C3d, C9neo) was occasionally detected in the lumen of blood vessels and in reactive astrocytes in brain tissue remote from the ventricles. Perivascular deposits of complement or the appearance of fibrous tissue within perivascular spaces were not seen in intact white or grey matter in any of the many sections studied. Instances in which deposits of activated complement were observed in distant brain tissue included, as mentioned above, an infarct of 67 h duration and an expanding early pre-phagocytic MS lesion.

Renal and Retinal Filtration Membranes

Filtration membranes in the kidney, behind the retina and in choroid plexus villi consist of similarly arranged membranes and fluid spaces subtending unusually large, leaky fenestrated capillaries (Fig. 13). Comparing the changes observed in choroid plexus filtration membranes in IFCP with those affecting filtration membranes in the retina in AMD and glomerular filtration membranes in age-related and immune complex renal diseases showed broadly similar pathological changes in basement membranes, capillaries and in the respective epithelial monolayers (choroid plexus epithelium, retinal pigmentary epithelium, podocytes) including intrusion of ridges of grossly thickened subepithelial basal laminae into the foot process zone of the overlying epithelium (Fig. 14). Important differences that were observed were, first, an absence of any EM evidence in IFCP of immune complex deposition as seen in immune complex renal diseases (Fig. 15), and, second, the presence, in only, of the unusual extracellular electron-dense material described earlier. Nothing similar was observed in the glomerular filtration membrane in any of the other renal biopsies examined electron microscopically or in the single retinal lesions examined in AMD.

DISCUSSION

The terms, "stromal" or "interstitial" fibrosis of the choroid plexus refer to the appearance of increasing amounts

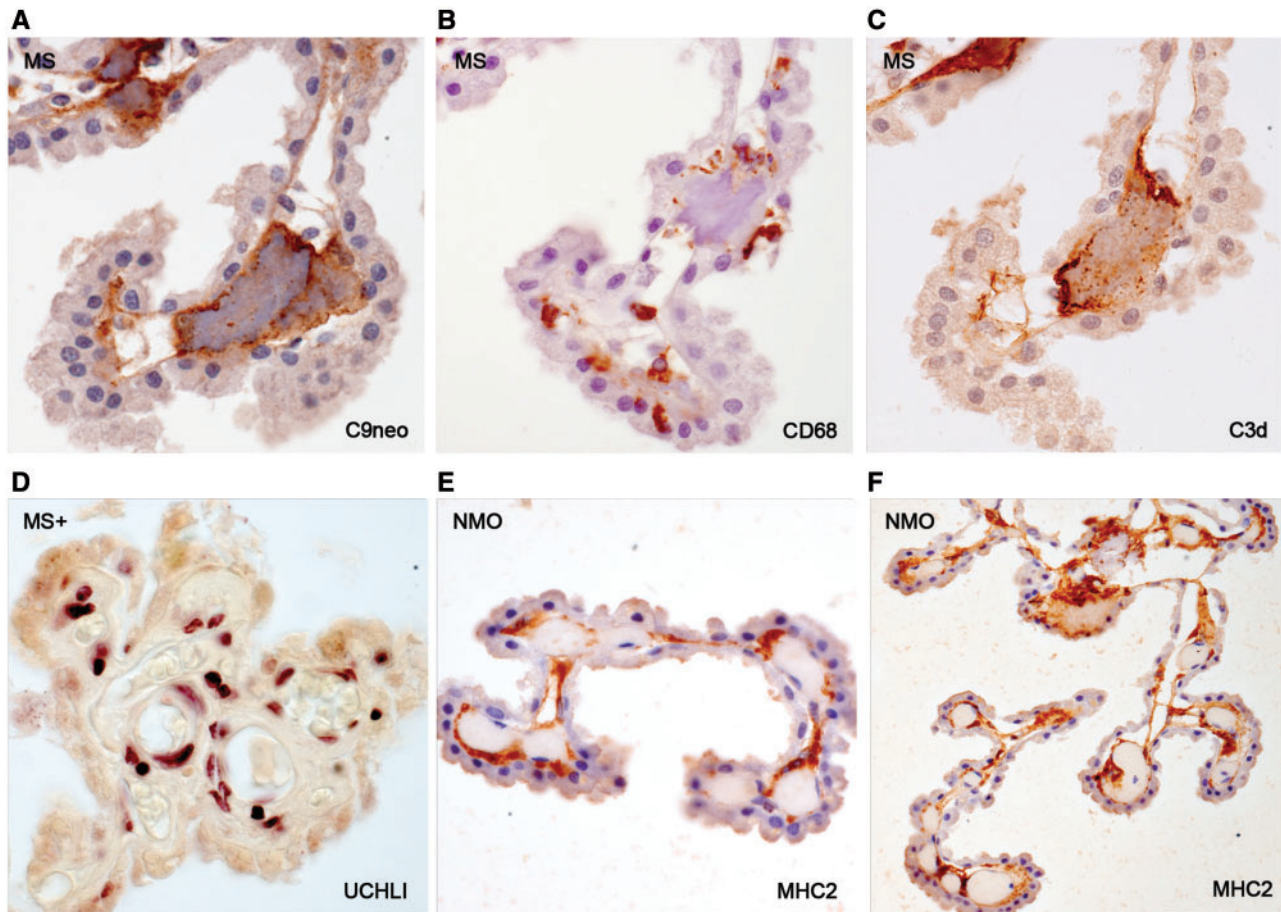


FIGURE 9. Inflammatory cells. In the choroid plexus of a patient with MS, a villous nodule contains a mineral inclusion (**A**). CD68-positive putative macrophages (**B**), although present close to complement-positive material, are unreactive for complement (**C**). (**D**) UCHL1-positive lymphocytes are numerous in the choroid plexus of a patient with MS and perivenous encephalomyelitis; the latter followed injections of pig brain given as a treatment for MS. (**E**, **F**) MHC2-positive cells are present throughout pericapillary spaces in a patient with NMO. **A**, C9neo; **B**, CD68; **C**, C3d; **D**, UCHL1; **E**, **F**, MHC2. Magnifications: **A–C**, **E**, **F**, $\times 320$; **D**, $\times 400$; **F**, $\times 180$.

of connective tissue, often forming nodules, within the normally narrow pericapillary space separating the capillary endothelium from the overlying epithelial monolayer of a choroid plexus villous; this appearance was likened by Adams and Sidman to the fibrosis and hyalinization of renal glomeruli that may be seen with advancing age (10).

Interstitial fibrosis and other changes in the choroid plexus including the presence of psammoma bodies, ring-like, silver-positive epithelial cell inclusions (“Biondi rings”), mineralized plate-like inclusions and xanthogranuloma commonly found in the aging brain are described in the current literature as “degenerative” in nature; and with no known physiological consequences (5, 10–18).

In an extensive review of the early literature, Cobb commented that the most common pathological change recognized to affect the choroid plexus in old age was “especially proliferation of the interstitial connective tissue”, and that in infants and early childhood “the layer of connective tissue between the epithelium and the capillaries is extremely thin, no more than ... a few connective tissue strands”; with age, these

increase in thickness to form larger masses of hyaline degeneration, which may calcify (11). Continuing, Cobb noted that, “with all these changes going on through life, it is very hard to know where normal ends and pathological (sic) begins. There is no perfectly unchanged choroid plexus except in healthy infants ... specimens from apparently normal children only 10 years of age and from young adults have ... regressive changes ... (which) in almost all chronic nervous diseases ... are found to an exaggerated degree”.

This study is the first study to demonstrate that the age-related change referred to by Cobb is associated with an innate inflammatory reaction located within the pericapillary space of the choroid plexus filtration membrane and that the presence of activated complement together with inflammatory cells in choroid plexus villi may be regarded as normal in adults, both in those with CNS disease (19, 20) and without CNS disease.

Other notable features of the lesion include: (i) destruction of capillaries; (1) the presence of unusual electron-dense particulate deposits (2). No similar deposits were observed in

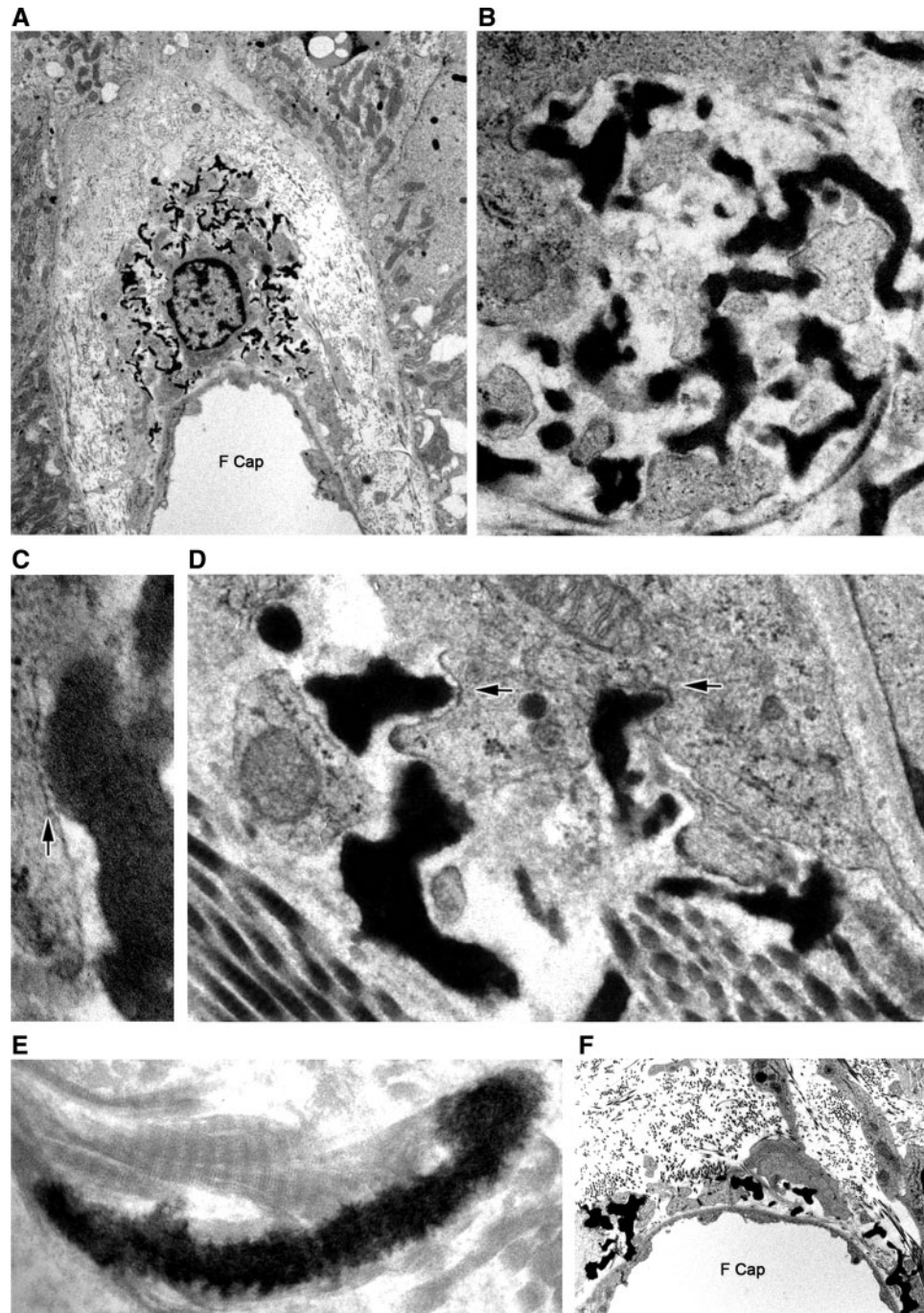


FIGURE 10. Electron photomicrographs of particulate electron-dense material in choroid plexus villi. **(A)** A cell located in the pericapillary space invests extracellular fragments of electron-dense material. **(B)** An area within the cell illustrated in panel A showing cell processes contacting but not endocytosing dark material. **(C, D)** Extracellular dark material contacts but is not endocytosed by perivascular cells. Arrows indicate points of contact with what appear to be clathrin-coated pits. **(E)** An elongated fragment of dark material roughly the size of adjacent collagen fibers. **(F)** Cell processes surround extracellular dark material located close to a villous capillary. **A**, $\times 2,900$; **B**, $\times 2,100$; **C**, $\times 68,200$; **D**, $\times 29,000$; **E**, $\times 64,400$; **F**, $\times 4,050$.

any of the renal diseases examined electron microscopically in the present study, or, as far as we could determine, reported in EM studies of drusen (5–9), which suggests that such material may be peculiar to IFCP); (iii) a failure by macrophages to

phagocytose extracellular aggregates of electron-dense matter. The inflammatory reaction is unusual in that, although CD68-positive, MHC2-positive, Fc-receptor- and complement receptor-bearing macrophages cluster around and contact the

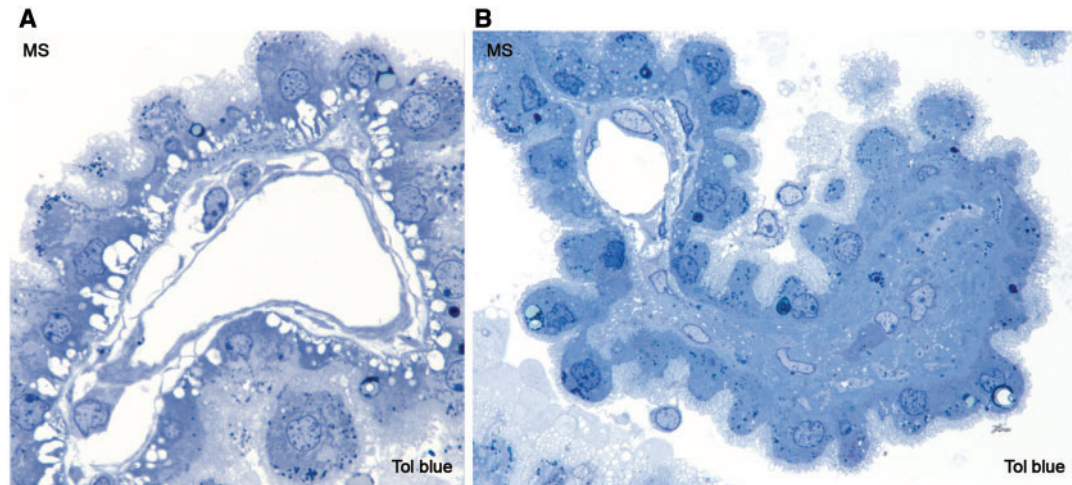


FIGURE 11. Interstitial fibrosis - capillary and epithelial damage in the choroid plexus of a 39-year-old woman with MS. **(A)** A semi-thin section of a choroid plexus villous in which the several components of the filtration membrane appear normal. The capillary endothelium is intact; there is a narrowly patent pericapillary space, and vacuoles corresponding to fluid-filled cistern located amongst epithelial cell foot processes are intact. **(B)** A semi-thin section of a villous in which the filtration membrane is replaced by marked stromal fibrosis. There is no centrally located capillary, the pericapillary space is gone, and the line of fluid cisterns at the base of the epithelial monolayer is no longer evident. There are 8 cells (a mixture presumably of fibroblasts and CD68-positive, MHC2-positive cells [nuclei only visible]) located within and around the nodule. **A, B**, toluidine blue, $\times 800$.

extracellular aggregates (21–23), there is no electron microscopic evidence of phagocytosis of the electron-dense material; (iv) damage to the choroid plexus epithelium that is restricted to changes at the basal absorptive surface of affected epithelial cells (loss of basal cisterns); and (v) no comparable age-associated inflammatory process in perivascular spaces where there is an intact blood-brain barrier, i.e. at mesenchymal-glia interfaces located within the parenchyma of the cerebrum (24).

Pathogenesis

That the IFCP lesion is due to immune complex deposition is unlikely because IgG was detected immunohistochemically in only half the cases, the staining pattern was the same in subjects with and without inflammatory diseases of the brain, and other serum proteins were sometimes present in the lesion. Also, neither in this study nor in a large number of EM studies of age-related changes affecting the choroid plexus has there been EM evidence of immune complex deposition of the sort diagnostic of immune complex disease in the kidney reported in (5–9).

A more likely possibility is that the inflammatory lesion in IFCP is related in some way to the still unknown process leading to tissue injury in AMD, FG and AD, 3 age-related diseases of uncertain cause; in all of these conditions, tissue injury is associated with an innate immune reaction directed at extracellular complement-reactive adventitious material of mixed molecular composition (25–29).

Shared morphological features that support this include the following: (i) A defining pathological characteristic of AD (17), AMD (30), FG (31) and IFCP is the presence of circumscribed extracellular deposits of filamentous and amorphous material of mixed molecular composition.

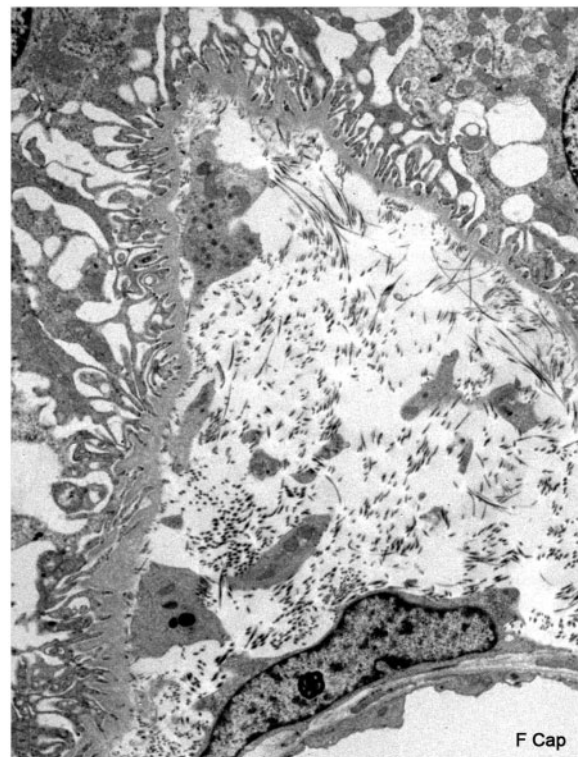


FIGURE 12. Interstitial fibrosis. There is widening of the pericapillary space in an affected choroid plexus villous. Commencing fibrosis is accompanied by thickening of the subepithelial basal lamina together with crowding and elongation of epithelial cell foot processes. Note the absence of evidence of immune complex deposition as seen in the kidney in Figure 15. F Cap, fenestrated capillary. Electron micrograph, $\times 3200$.

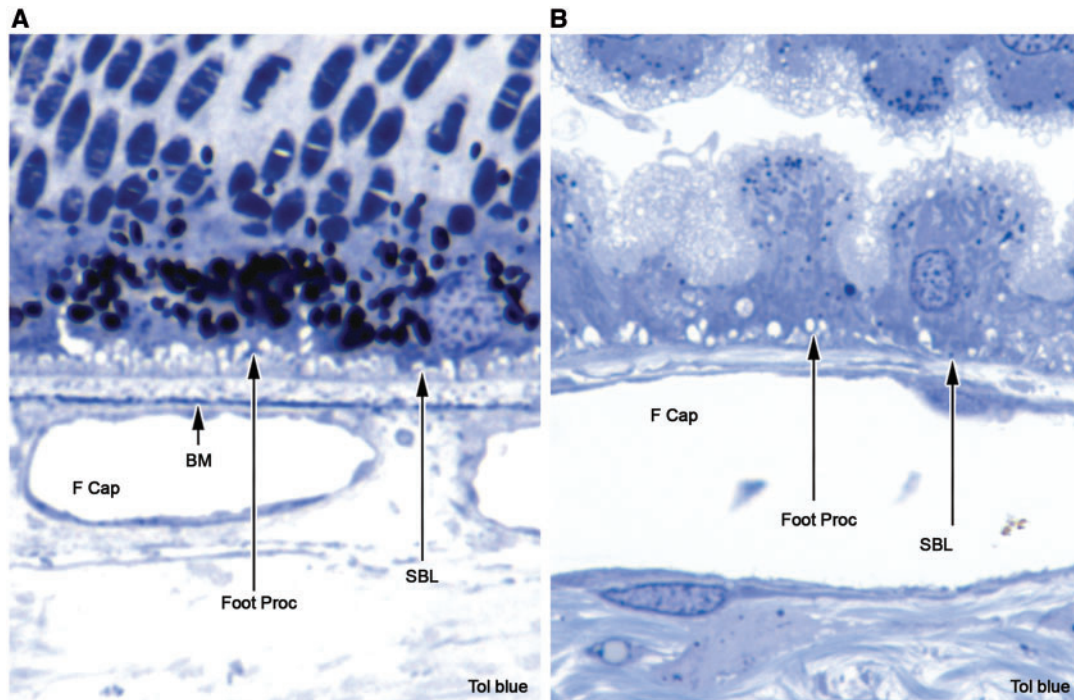


FIGURE 13. Filtration membranes. Semi-thin sections of retinal (left) and choroid plexus (right) filtration membranes showing fenestrated capillaries separated by a narrow pericapillary space from the absorptive zone of epithelial cell foot processes. Expanding inflammatory lesions within this space damage the overlying epithelial monolayer in AMD and in inflammation of choroid plexus villi. F cap, fenestrated capillary; BM, Bruch's membrane; Foot Proc, foot processes; SBL, subepithelial basement membrane. Toluidine blue; Magnifications: left, $\times 2200$; right, $\times 1500$.

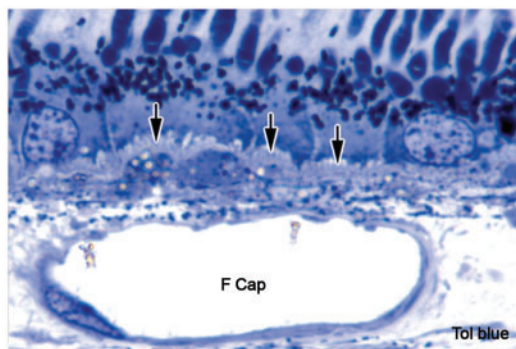


FIGURE 14. Age-related macular degeneration. The retinal filtration membrane in a patient with pathologically defined AMD. Nodules of drusen capped with a pale band of thickened basement membrane impinge on and displace upwards the retinal pigmentary epithelial cell layer (arrows). When compared with normal regions of the retinal filtration membrane (Fig. 13A), it is apparent that there is also some loss of the vacuolated absorptive foot process zone at the base of each epithelial cell. Such appearances indicate possible injury both to the pigmentary cell layer and to the epithelial monolayer. F Cap, fenestrated capillary. Semi-thin section, toluidine blue, $\times 2100$.

(ii) An important histopathological finding in IFCP, AMD and FG is the presence in each of a markedly thickened, PAS-positive subepithelial basal lamina that, together with deposited material, intrudes into and damages the basal absorptive surface

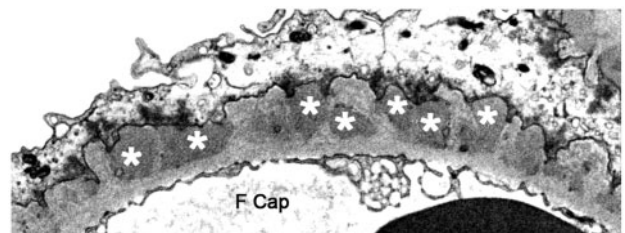


FIGURE 15. Renal immune complex disease. Immune complex deposition (asterisks) is associated with a thickly ridged renal glomerular basement membrane in a patient with membranous glomerulonephritis (stage 2). Electron micrograph, $\times 6200$.

of the overlying epithelium (31–34). This commonality is particularly impressive in AMD, which like IFCP, is defined as a filtration membrane disorder characterized by the presence of a thickened, redundant subepithelial basement membrane capping an extracellular dome-shaped complement-reactive amorphous deposit infiltrated by MHC2-activated mononuclear and other inflammatory cells (30, 32, 33, 35). (iii) The location of the deposits is somewhat similar in each of the 4 conditions. In AMD, IFCP and FG the deposits form within pericapillary spaces of open fenestrated capillaries in filtration membranes at the blood-CSF barrier (IFCP), at the blood-retina barrier (AMD), and at the blood-urinary barrier (FG). In the case of AD, extracellular material (senile plaques containing filamentous amyloid beta),

develop close to “leaky” capillaries in the capillary-rich cerebral cortex (18, 36–39). (iv) The lesions are inflammatory, with features indicative of an innate immune response directed at some component of an extracellular aggregate of unwanted material (32, 34, 35, 40–43); these findings lead to the inflammatory hypothesis of neural damage in AD and of photoreceptor damage in AMD (44, 45). In AD, the immunogen has been identified as β -amyloid or amyloid oligomers (46). The immunogen is unknown in AMD (27, 29, 34, 35, 42) and in IFCP (25). It is possible that the extracellular electron-dense material peculiar to IFCP may be an immunogen and that this material may be to IFCP what β -amyloid is to AD. (v) The deposits are not benign but are associated with capillary damage and loss as well as changes in nearby structures (36, 37). How the deposits cause damage is uncertain. One theory, common to AD, AMD and FG, and that may apply to IFCP favors injury by toxic inflammatory mediators including those associated with frustrated phagocytosis. (vi) Failure of clearance mechanism. There are several important theories regarding the origin of extracellular deposits in AD and in AMD. One theory invokes a failure by macrophages to phagocytose and degrade the deposits, i.e. a failure by macrophages to clear adventitious β -amyloid in AD and drusen in the case of AMD (16, 17, 32, 34, 41–43, 47–54). The same mechanism may be responsible for the accumulation of adventitious material (electron-dense material) in the choroid plexus in IFCP. The present finding of what appears to be failed clathrin-mediated endocytosis by macrophages engaging electron-dense deposited material in affected villi may support this. There is evidence of a similar failure of clathrin-mediated endocytosis by clustered microglia engaging the pointed ends of bundles of β -amyloid filaments in AD (18, 54).

Paraffin sections immunostained for complement show no reactivity anywhere in the brain or in associated tissues in young subjects without neurological disease. In many individuals, with increasing age, conspicuous immunoreactive deposits of complement begin appearing in 3 locations: in association with extracellular amyloid deposits in AD, extracellular deposits of drusen in AMD, and the yet to be characterized extracellular electron-dense particulate matter in choroid plexus villi. Common factors such as the capillary lesion, the location of deposits near capillaries or in filtration membranes, or frustrated phagocytosis, in addition to the composition of the deposits, may play a role in the pathogenesis of IFCP, AMD and AD.

Clinical Significance

Whereas it is likely that the structural changes in IFCP have physiological consequences, in view of the range of activities the choroid plexus and the CSF play in development, homeostasis, control of brain and cerebrospinal fluid volume, and neuronal repair (55, 56), there is no evidence at this time that the changes described are clinically significant. This has not been tested, however, because no biomarker has been identified for the condition and it remains to be seen whether there are clinical deficits associated with IFCP (17, 26, 55).

Summary

Textbook accounts of the normal human choroid plexus draw on findings in young animals and children (57). These describe pristine choroid plexus villi, each one occupied almost entirely by a single large capillary and a virtually empty pericapillary space (6, 9, 17, 57, 58). In the present study, almost everyone except children showed this space to be occupied to varying degrees by an innate inflammatory process accompanied by destruction of the capillary bed and alterations to the overlying choroid plexus epithelium. Structural changes were identified that resemble those affecting the retinal filtration membrane in subjects with AMD, the renal filtration membrane in subjects with an age-related renal disease, and Alzheimer disease.

ACKNOWLEDGMENTS

We would like to thank Professor B.P. Morgan for complement antibodies, Professor C Harper for providing tissue from the University of Sydney brain bank, Professors P Amati and J. Pollard for helpful discussion, and Dr. R.J. Prineas and Dr. C. Stevens for help with the statistical analysis. Technical assistance was provided by Eunice Kwon, Toan Nguyen, Hung Jiew Lee and Stephen Kum-Jew.

REFERENCES

- Parratt JD, Prineas JW. Neuromyelitis optica: a demyelinating disease characterized by acute destruction and regeneration of perivascular astrocytes. *Mult Scler* 2010;16:1156–72
- Misu T, Fujihara K, Kakita A, et al. Loss of aquaporin 4 in lesions of neuromyelitis optica: distinction from multiple sclerosis. *Brain* 2007;130:1224–34
- Roemer SF, Parisi JE, Lennon VA, et al. Pattern-specific loss of aquaporin-4 immunoreactivity distinguishes neuromyelitis optica from multiple sclerosis. *Brain* 2007;130:1194–205
- Prineas JW. Multiple sclerosis: presence of lymphatic capillaries and lymphoid tissue in the brain and spinal cord. *Science* 1979;203:1123–5
- Adams RD, Oksche A, Haymaker W. Meninges, choroid plexuses, ependyma and their reactions. Part 2: Age-related changes and pathology. In: Haymaker W, Adams RD, eds. *Histology and Histopathology of the Nervous System*. Springfield, IL: Charles C. Thomas 1982:641–713
- Nag S. The ependyma and choroid plexus. In: Davis RL, Robertson DM, eds. *Textbook of Neuropathology*, 2nd edn. Baltimore, MD: Williams and Wilkins 1991:95–114
- Dunn J Jr, Kernohan JW. Histologic changes within the choroid plexus of the lateral ventricle: their relation to age. *Proc Staff Meet Mayo Clin* 1955;30:607–16
- Millen JW, Woollam DHM. *The Anatomy of the Cerebrospinal Fluid*. London, New York, Toronto: Oxford University Press, 1962
- Bargmann W, Oksche A, Haymaker W, et al. Meninges, choroid plexuses, ependyma and their reactions. Part 1: Histology and Functional Considerations. In: Haymaker W, Adams RD, eds., *Histology and Histopathology of the Nervous System*. Charles C. Thomas Springfield, IL 1982:560–641
- Adams RD, Sidman RL. *Introduction to Neuropathology*. New York, Toronto, Sydney, London: McGraw-Hill 1968
- Cobb S. The cerebrospinal blood vessels. In: Penfield W, ed. *Cytology and Cellular Pathology of the Nervous System*. Vol. 2. New York: Paul B. Hoeber 1932:577–610
- Corsellis JAN. Aging and the dementias. In: Blackwood W, Corsellis JAN, eds. *Greenfield's Neuropathology*. London: Edward Arnold, 1976: 796–848
- Banati RB, Beyreuther K. Alzheimer's disease. In: Kettenmann H, Ransom BR, eds. *Neuroglia*. New York: Oxford University Press 1995: 1027–43

14. Mrak RE, Griffin ST, Graham DI. Aging-associated changes in human brain. *J Neuropathol Exp Neurol* 1997;56:1269–75
15. Esiri MM, Hyman BT, Beyreuther K, et al. Ageing and dementia. In: Graham DI, Lantos PL, eds. *Greenfield's Neuropathology*, 6th edn. London, Sydney, Auckland: Arnold 1997:153–233
16. Graeber MB, Blakemore WF, Kreutzberg GW. Cellular pathology of the central nervous system. In: Graham DI, Lantos PL, eds. *Greenfield's Neuropathology*, 7th edn. London, New York, Delhi: Arnold 2002:123–91
17. Lowe J, Mirra SS, Hyman BT, et al. Ageing and dementia. In: Love S, Louis DN, Ellison DW, eds. *Greenfield's Neuropathology*, 8th edn. London: Hodder Arnold 2008:1031–152
18. Vinters HV, Kleinschmidt-Demasters BK. General pathology of the central nervous system. In: Love S, DN Louis DN, DW Ellison DW, eds. *Greenfield's Neuropathology*, 8th edn. London: Hodder Arnold 2008:1–62
19. Lampert PW, Oldstone MB. Host immunoglobulin G and complement deposits in the choroid plexus during spontaneous immune complex disease. *Science* 1973;180:408–10
20. Vercellino M, Votta B, Condello C, et al. Involvement of the choroid plexus in multiple sclerosis autoimmune inflammation: a neuropathological study. *J Neuroimmunol* 2008;199:133–41
21. Braathen LR, Forre OT, Husby G, et al. Evidence for Fc receptors and complement factor C3b receptors in human choroid plexus. *Clin Immunol Immunopathol* 1979;14:284–93
22. Peress NS, Roxburgh VA, Gelfand MC. Binding sites for immune components in human choroid plexus. *Arthritis Rheum* 1981;24:520–6
23. Nyland H. Properties of Fc receptors in the human nervous system. *Acta Pathol Microbiol Immunol Scand* 1982;C90:171–7
24. Prineas JW, Wright RG. Macrophages, lymphocytes, and plasma cells in the perivascular compartment in chronic multiple sclerosis. *Lab Invest* 1978;38:409–21
25. Eriksson L, Westermark P. Intracellular neurofibrillary tangle-like aggregations. A constantly present amyloid alteration in the aging choroid plexus. *Am J Pathol* 1986;125:124–9
26. Silverberg GD, Mayo M, Saul T, et al. Alzheimer's disease, normal-pressure hydrocephalus and senescent changes in CSF circulatory physiology: a hypothesis. *Lancet Neurol* 2003;2:506–11
27. Ohno-Matsui K. Parallel findings in age-related macular degeneration and Alzheimer's disease. *Prog Retin Eye Res* 2011;30:217–38
28. Krzyzanowska A. Pathological alteration in the choroid plexus of Alzheimer's disease: implication for new therapy approaches. *Front Pharmacol* 2012;3:75
29. Sivak JM. The aging eye: common degenerative mechanisms between the Alzheimer's brain and retinal disease. *Invest Ophthalmol Vis Sci* 2013;54:871–80
30. Curcio CA, Johnson M. Structure, function and pathology of bruch's membrane. In: Hilton D, ed. *Retina*, 5th edn. London: Elsevier 2012:465–81
31. Rosenstock JL, Markowitz GS, Valeri AM, et al. Fibrillary and immunotactoid glomerulonephritis: distinct entities with different clinical and pathologic features. *Kidney Int* 2003;63:1450–61
32. Baudouin C, Peyman GA, Fredj-Reygrobelle D, et al. Immunohistochemical study of subretinal membranes in age-related macular degeneration. *Jpn J Ophthalmol* 1992;36:443–51
33. Sarks SH, Arnold JJ, Killingsworth MC, et al. Early drusen formation in the normal and aging eye and their relation to age related maculopathy: a clinicopathological study. *Br J Ophthalmol* 1999;83:358–68
34. Johnson LV, Leitner WP, Staples MK, et al. Complement activation and inflammatory processes in Drusen formation and age related macular degeneration. *Exp Eye Res* 2001;73:887–96
35. Van der Schaft TL, Mooy CM, de Bruijn WC, et al. Early stages of age-related macular degeneration: an immunofluorescence and electron microscopy study. *Br J Ophthalmol* 1993;77:657–61
36. Stewart PA, Hayakawa K, Akers MA, et al. A morphometric study of the blood-brain barrier in Alzheimer's disease. *Lab Invest* 1992;67:734–42
37. Bowman GL, Kaye JA, Moore M, et al. Blood-brain barrier impairment in Alzheimer's disease: stability and functional significance. *Neurology* 2007;68:1809–14
38. Ryu JK, McLarnon JG. A leaky blood-brain barrier, fibrinogen infiltration and microglial reactivity in inflamed Alzheimer's disease brain. *J Cell Mol Med* 2009;13:2911–25
39. Pluta R. Is the ischemic blood-brain barrier insufficiency responsible for full-blown Alzheimer's disease? *Neurol Res* 2006;28:665–71
40. McGeer PL, Rogers J, McGeer EG. Inflammation, anti-inflammatory agents and Alzheimer disease: the last 12 years. *J Alzheimers Dis* 2006;9:271–6
41. El Khoury J, Hickman SE, Thomas CA, et al. Microglia, scavenger receptors, and the pathogenesis of Alzheimer's disease. *Neurobiol Aging* 1998;19:S81–4
42. Shi J, Wang Q, Johansson JU, et al. Inflammatory prostaglandin E2 signaling in a mouse model of Alzheimer's disease. *Ann Neurol* 2012;72:788–98
43. Liu RT, Gao J, Cao S, et al. Inflammatory mediators induced by amyloid-beta in the retina and RPE in vivo: implications for inflammatory activation in age-related macular degeneration. *Invest Ophthalmol Vis Sci* 2013;54:2225–37
44. McGeer PL, Kawamata T, Walker DG, et al. Microglia in degenerative neurological disease. *Glia* 1993;7:84–92
45. Schwab C, Steele JC, McGeer PL. Neurofibrillary tangles of Guam parkinson-dementia are associated with reactive microglia and complement proteins. *Brain Res* 1996;707:196–205
46. Glabe CG, Kaye R. Common structure and toxic function of amyloid oligomers implies a common mechanism of pathogenesis. *Neurology* 2006;66:S74–8
47. Weller RO, Subash M, Preston SD, et al. Perivascular drainage of amyloid-beta peptides from the brain and its failure in cerebral amyloid angiopathy and Alzheimer's disease. *Brain Pathol* 2008;18:253–66
48. Mawuenyega KG, Sigurdson W, Ovod V, et al. Decreased clearance of CNS beta-amyloid in Alzheimer's disease. *Science* 2010;330:1774
49. Roberts KF, Elbert DL, Kasten TP, et al. Amyloid-beta efflux from the central nervous system into the plasma. *Ann Neurol* 2014;76:837–44
50. Wang YJ, Zhou HD, Zhou XF. Clearance of amyloid-beta in Alzheimer's disease: progress, problems and perspectives. *Drug Discov Today* 2006;11:931–8
51. Kress BT, Iliff JJ, Xia M, et al. Impairment of paravascular clearance pathways in the aging brain. *Ann Neurol* 2014;76:845–61
52. May C, Kaye JA, Atack JR, et al. Cerebrospinal fluid production is reduced in healthy aging. *Neurology* 1990;40:500–3
53. Mirra SS, Hart MN, Terry RD. Making the diagnosis of Alzheimer's disease. A primer for practicing pathologists. *Arch Pathol Lab Med* 1993;117:132–44
54. Mirra SS, Hyman BT. Ageing and dementia. In: Graham DI, Lantos PL, eds. *Greenfield's Neuropathology*, 7th edn, London: Hodder Arnold, 2002:212
55. Redzic ZB, Preston JE, Duncan JA, et al. The choroid plexus-cerebrospinal fluid system: from development to aging. *Curr Top Dev Biol* 2005;71:1–52
56. Daneman R. The blood-brain barrier in health and disease. *Ann Neurol* 2012;72:648–72
57. Peters A, Palay SL, Webster H. dF. The fine structure of the nervous system. In: *The Neurons and Supporting Cells*. Philadelphia: WB Saunders, 1976:280–94
58. Reichenbach A, Robinson SR. Ependymoglia and ependymoglia-like cells. In: Kettenmann H, Ransom BR, eds. *Neuroglia*. New York: Oxford University Press 1995:58–84